Journal of Statistics & Management Systems
ISSN 0972-0510 (Print), ISSN 2169-0014 (Online)
Vol. 29 (2026), No. 2, pp. 111–133
DOI : 10.47974/JSMS-1358

Extension of the heavy-tailed distribution with applications in medical sciences

Simbarashe Chamunorwa *
Department of Mathematics and Statistical Sciences
Botswana International University of Science and Technology
Palapye
Botswana

and

Department of Applied Statistics
Manicaland State University of Applied Sciences
Mutare
Zimbabwe

Broderick Oluyede †
Fastel Chipepa §
Kethamile Ranonna ‡
Department of Mathematics and Statistical Sciences
Botswana International University of Science and Technology
Palapye
Botswana

Abstract

Heavy-tailed-Type II Exponentiated Half Logistic-Gompertz-G (HT-TIIExHL-G-G) class of distributions is proposed in this article. The structural properties of the distribution are thoroughly explored, and specific cases within this family are presented. We carried out simulation study to explore the estimation of the model parameters through several established techniques. The analysis showcased their numerical efficiency and performance. Furthermore, through the utilization of maximum likelihood technique, we use a specific instance from the HT-TIIExHL-G-G family of distributions (FD) to show its practical

* *E-mail:* **CS19100117@biust.ac.bw; (Corresponding Author)**
simbarashe.chamunorwa@staff.msuas.ac.zw
† *E-mail:* **oluyedeo@biust.ac.bw**
§ *E-mail:* **chipepaf@biust.ac.bw**
‡ *E-mail:* **RK15000146@biust.ac.bw**

application. This is achieved by fitting it to three real-world data examples from health care and engineering disciplines.

Subject Classification (2010): *60E05, 62E15, 62F30.*

Keywords: *Heavy-tailed distribution, Exponentiated distribution, Gompertz distribution, Simulations, Maximum likelihood estimation.*

1. Introduction

Emerging communicable diseases are important challenges in the recent years. A current outbreak of coronavirus pneumonia (Covid-19), is a wake-up call for the need to improve global health security. Statistical modeling of such diseases are important in our life as it is crucial for researchers to understand the behavior of the spread of each virus and its effect on humanity. As usual, various medical datasets are typically positive and unimodal, with a hump-shaped distribution and heavier tails than classical models. Classical distributions have some limitations, due to the fact that they are not sufficiently versatile to offer the optimal fit to datasets with Heavy tails. For instance, in health science research, the length of stay in hospitals has been shown to have a highly skewed, heavy-tailed distribution (Ickowicz and Sparks [8] and Harini et al. [7]). This means that the distribution is not symmetrical, with a long tail of extreme values. As a result, the standard classical distributions, such as the normal distribution, are not able to provide an adequate fit to this data.

Scientists have studied heavy-tailed distributions to explore several aspects of real lifetime problems. The literature has offered a variety of other recent distributions, including the work by [14], [15], [1] and [3]. One of the distributions with many applications in several fields, including but not limited to medical sciences, actuary science, biology, gerontology, and survival analysis, is the Gompertz distribution by Gompertz [6]. The Gompertz distribution has recently undergone improvements that have enhanced its adaptability and ability to model various life time data sets. Extensions of the Gompertz distribution include work by [2], [3], [9], [11] and [23].

In addition to what we have discussed above, it is well known that classical statistical distributions fail to capture important characteristics of world data sets that display extreme values-based behavior and produces long tails. In similar circumstances, classical models are not the most ideal choice to apply (see Dutta and Perry [5] for more details).

Our motivation is inspired by the development of flexible generalized FD which provide better fits utilizing data modeling with more precision. In this regard, we are attracted by the applicability of the extended and generalized heavy-tailed and Gompertz distributions in many fields. Thus, we introduced the HT-TIIExHL-G-G FD. This study is dedicated to exploring both the theoretical and practical aspects, with a particular focus on the practical applications. In fact, a significant part is devoted to the parameter estimation of the model through a range of methods, encompassing all the details. The new FD offers more flexibility and can be applied to a wider range of applications such as medical sciences and other research areas for some data sets when compared to selected distributions.

The following is how the paper is set up: Section 2 introduces the new FD and some of its statistical properties. Section 3 presents seven different parameter estimation techniques for the HT-TIIExHL-G-G FD. In Section 4, actuarial metrics are provided. A few unique cases of the newly described FD are given in Section 5. A simulation study is presented in Section 6, and applications are covered in Section 7. Conclusions are made at the end of the paper.

2. New Family

Within this section, the authors introduce the HT-TIIExHL-G-G FD. We also derive some structural properties of this new distribution.

2.1 The New Distribution

In this work, we combine two transformations, the heavy-tailed FD developed by Zhao et al. [15], and the type II exponentiated half logistic-Gompertz-G FD by Oluyede et al. [10]. Utilizing the aforementioned distributions, the proposed HT-TIIExHL-G-G FD cumulative density function cdf and probability density function (pdf) are provided by

$$F(x;\alpha,\sigma,\omega,\Lambda) = 1-\left(\frac{D}{1-(1-\sigma)(1-D)}\right)^{\sigma} \tag{2.1}$$

and

$$\begin{aligned} f(x;\alpha,\sigma,\omega,\Lambda) &= 2\,\alpha\sigma^2 g(x;\Lambda) e^{\left(\frac{\alpha\sigma}{\omega}\{1-[1-G(x;\Lambda)]^{-\omega}\}\right)}[1-G(x;\Lambda)]^{-\omega-1} \\ &\times \left(1+\left[1-e^{\left(\frac{1}{\omega}\{1-[1-G(x;\Lambda)]^{-\omega}\}\right)}\right]\right)^{-\alpha\sigma-1} \\ &\times\ [1-(1-\sigma)(1-D)]^{-(\sigma+1)}, \end{aligned} \tag{2.2}$$

respectively, for $\alpha,\sigma,\omega>0$, where $D=\left[\frac{e^{(\frac{1}{\omega}(1-[1-G(x;\Lambda)]^{-\omega}))}}{1+(1-e^{(\frac{1}{\omega}(1-[1-G(x;\Lambda)]^{-\omega}))})}\right]^{\alpha}$ and baseline parameter vector Λ and parameter vector Λ from the baseline distribution.

2.2 *Inverse Distribution Function*

The function that calculates quantiles for the HT-TIIExHL-G-G FD is given as

$$Q_X(z) = G^{-1}\left(1-\left[1-\omega\ln\left(\frac{2\left[\frac{\sigma(1-z)^{1/\sigma}}{1-(1-z)^{1/\sigma}+\sigma(1-z)^{1/\sigma}}\right]^{1/\alpha}}{1+\left[\frac{\sigma(1-z)^{1/\sigma}}{1-(1-z)^{1/\sigma}+\sigma(1-z)^{1/\sigma}}\right]^{1/\alpha}}\right)\right]^{-1/\omega}\right). \tag{2.3}$$

If we specify the baseline cdf G, random numbers from the HT-TIIExHL-G-G FD can be generated using equation (2.3).

2.3 *Linearization*

We provide series expansion of the HT-TIIExHL-G-G FD. The pdf, as described in equation (2.2), can be represented as follows:

$$f(x;\alpha,\sigma,\omega,\Lambda) = \sum_{q=0}^{\infty} \eta_{q+1} g_{q+1}(x;\Lambda),$$

where $g_{q+1}(x;\Lambda) = (q+1)g(x;\Lambda)G^{q}(x;\Lambda)$ represents the exponentiated-G (exp-G) distribution's density function with a power parameter of $(q+1)$ and

$$\eta_{q+1} = \sum_{h,i,j,k,l,m,p=0}^{\infty} \frac{(-1)^{h+i+q+p+k}(1-\sigma)^{h}(\alpha(i+\sigma)+k)^{l}}{\omega^{l} l!(q+1)} 2\alpha\sigma^{2} \binom{-(\sigma+1)}{h}\binom{h}{i} \times \binom{-\alpha(i+\sigma)-1}{j}\binom{l}{p}\binom{j}{k}\binom{-\omega(1+p)-1}{q}. \quad (2.4)$$

As a result, the structural properties of the HT-TIIExHL-G-G FD is deduced using the same characteristics of the Exp-G distribution. Please refer to the appendix for more information on the derivations.

2.4 *Characteristic Function*

Given that X follows the HT-TIIExHL-G-G model and Y follows the $Exp-G(q+1)$ distribution. The r^{th} moment, μ_r' of the HT-TIIExHL-G-G FD is computed as

$$\mu_r' = E(X^r) = \int_{-\infty}^{\infty} x^r f(x;\alpha,\sigma,\omega,\Lambda)dx = \sum_{q=0}^{\infty} \eta_{q+1} E(Y^r),$$

where η_{q+1} is provided in equation (2.4). The characteristic function $M(t)$=$E(e^{tX})$, is expressed as

$$M_X(t) = \sum_{q=0}^{\infty} \eta_{q+1} M_Y(t),$$

where, $M_Y(t)$ represents the moment generating function of the random variable (rv) Y, and η_{q+1} is obtained from equation (2.4).

2.5 *Rényi's Uncertainty Measure and Order Statistics*

We used the HT-TIIExHL-G-G FD to compute the Rényi entropy and the probability distribution of the k^{th} order statistic.

2.5.1 Entropy

We present the Rényi entropy for the HT-TIIExHL-G-G FD. Entropy serves as a quantification of uncertainty or variability associated with a rv. The Rényi entropy for HT-TIIExHL-G-G FD is given by

$$I_R(\nu) = \frac{1}{1-\nu} \ln\left(\sum_{p=0}^{\infty} U_p^{*} e^{(1-\nu)\int_0^{\infty}[(1+p/\nu)g(x;\Lambda)G^{p/\nu}(x;\Lambda)]^{\nu}dx}\right),$$

For a detailed derivations, please refer to the appendix.

2.5.2 Order Statistics

Let us examine a set of n rv's that are iid following the HT-TIIExHL-G-G distribution. When we arrange these variables in increasing order yields the order statistics $X_{1:n} < X_{2:n} \ldots < X_{n:n}$. The k^{th} order statistic has the following pdf

$$f_{k:n}(x) = \sum_{w=0}^{\infty} C_{w+1} g_{w+1}(x;\Lambda), \tag{2.5}$$

where $g_{w+1}(x;\Lambda) = (w+1)g(x;\Lambda)G^{w}(x;\Lambda)$ denotes the pdf of the exponentiated-G distribution with a power parameter of $(w+1)$ and linear component

$$C_{w+1} = \frac{n!}{(k-1)!(n-k)!} \sum_{j=0}^{n-k} \sum_{n=1}^{\infty} \sum_{h,i,l,m,p,q,s=0}^{\infty} \frac{2\sigma^2 \alpha(1)^{j+h+i+l+p+s+w}(1-\sigma)^{i}(\alpha(l+\sigma)+p)^{q}}{\omega^{q} q!(w+1)}$$
$$\times \binom{j+k-1}{h}\binom{-\sigma(h+1)-1}{i}\binom{i}{l}\binom{-\alpha(l+\sigma)-1}{m}\binom{m}{p}\binom{q}{s}$$
$$\times \binom{-\omega(s+1)-1}{w}. \tag{2.6}$$

The t^{th} moment of the k^{th} order statistic from the HT-TIIExHL-G-G FD distribution is derived from equation (2.6). Refer to the appendix for a detailed derivation of the k^{th} order statistic.

3. Estimation Techniques

In statistical analysis, the process of estimating the values of unknown parameters based on a provided sample holds significant importance. Within this section, we focus on estimating the uncertain parameters of the HT-TIIExHL-G-G FD. This estimation is facilitated through the utilization of seven distinct estimation techniques such as maximum likelihood (MLE), maximum product spacings (MPS), Anderson Darling (AD), right tail Anderson Darling (RADE), least squares (LS), weighted least square (WLS) and Cramér Von Mises (CVM). See the appendix for more details.

4. Actuarial Measures

Actuarial and financial organizations frequently employ key risk indicators to manage their exposures to complex risks. We will discuss some crucial risk management strategies for the HT-TIIExHL-G-G FD.

4.1 *Value at Risk*

The VaR of a rv X is defined as the u^{th} quantile of its cdf. When X follows the probability distribution HT-TIIExHL-G-G FD, the VaR of X, denoted as VaR_z, can be expressed as follows:

$$VaR_z = x_z = G^{-1}\left(1 - \left[1 - \omega \ln\left(\frac{2\left[\frac{\sigma(1-z)^{1/\sigma}}{1-(1-z)^{1/\sigma}+\sigma(1-z)^{1/\sigma}}\right]^{1/\alpha}}{1+\left[\frac{\sigma(1-z)^{1/\sigma}}{1-(1-z)^{1/\sigma}+\sigma(1-z)^{1/\sigma}}\right]^{1/\alpha}}\right)\right]^{-1/\omega}\right),$$

for $0 < z < 1$.

4.2 *Tail Value at Risk*

The TVaR measures the expected loss given that an event beyond a specified probability level has occurred. For the HT-TIIExHL-G-G FD, the TVaR is characterized as follows:

$$\begin{aligned} TVaR_z &= \frac{1}{1-z}\int_{VaR_z}^{\infty} xf(x;\alpha,\sigma,\omega,\Lambda)dx \\ &= \frac{1}{1-z}\sum_{r=0}^{\infty} \eta_{r+1}\int_{VaR_z}^{\infty} xg_{r+1}(x;\Lambda)dx. \end{aligned} \tag{4.1}$$

In this context, the exp-G distribution is defined as having a power parameter of $(r+1)$, and it is represented by $g_{r+1}(x;\Lambda) = (r+1)g(x;\Lambda)G^r(x;\Lambda)$, where η_{r+1} is given by equation (2.4). Therefore, the TVaR of the HT-TIIExHL-G-G FD is determined using the exp-G distribution.

4.3 *Tail Variance*

For the HT-TIIExHL-G-G FD, can be obtained through the following derivation:

$$\begin{aligned} TV_z &= E(X^2|X > x_z) - (TVaR_z)^2 \\ &= \frac{1}{1-z}\int_{VaR_z}^{\infty} x^2 f(x;\alpha,\sigma,\omega,\Lambda)dx - (TVaR_z)^2 \\ &= \frac{1}{1-z}\sum_{r=0}^{\infty} \eta_{r+1}\int_{VaR_z}^{\infty} x^2 g_{r+1}(x;\Lambda)dx - (TVaR_z)^2, \end{aligned} \tag{4.2}$$

In this case, the exp-G distribution is defined as having a power parameter of $(r+1)$, and it is represented by $g_{r+1}(x;\Lambda) = (r+1)g(x;\Lambda)G^r(x;\Lambda)$, where η_{r+1} is provided by equation (2.4). Therefore, the TV of the HT-TIIExHL-G-G FD is determined using the exponentiated-G model.

4.4 *Tail Variance Premium*

The TVP of the HT-TIIExHL-G-G distribution can be calculated as

$$TVP_z = TVaR_z + \sigma(TV_z),$$

for $0 < \sigma < 1$. Using equations (4.1) and (4.2), we get the TVP of the HT-TIIExHL-G-G FD.

4.5 *Risk Assessment Simulations*

In this subsection, we conducted a numerical study of the VaR, TVaR, TV, and TVP measures. We compared the risk measures of the HT-TIIExHL-G-W distribution to those of the exponentiated odd Weibull-Topp Leone-log-logistic (EOWTLL), Heavy Tailed-Gompertz-Weibull (HT-Gom-W), alpha power exponentiated log-logistic (APExLLD), Type II Exponentiated Half Logistic-Gompertz-W (EHL-Gom-W), Gompertz-Weibull (Gom-W), Type II Exponentiated Half Logistic-W (TIIEHL-W), Weibull (W), and type 1 Heavy Tailed-Weibull (TIHT-W) distributions for various sets of parameters.

To assess the tail heaviness of the distributions, we employed the maximum likelihood method to estimate the parameters of the HT-TIIExHL-G-W and other mentioned distributions. Random samples of size $n = 100$ were generated from each distribution, and the estimation process was repeated 1000 times. Subsequently, we calculated the Value at Risk (VaR), Tail Value at Risk (TVaR), Tail Variance (TV), and Tail Probability (TVP) for each distribution.

The numerical results of these risk measures are summarized in Table 1. HT-TIIExHL-G-W model consistently yields higher values for the risk measures compared to the other distributions as shown in findings presented in Table 1. This suggests that the HT-TIIExHL-G-W distribution possesses a heavier tail in comparison.

Table 1
Risk Assessment Simulations

Distribution	Significance level	VaR	TVaR	TV	TVP
	0.70	0.1323	8.5657	626.8696	447.3744
HT-TIIExHL-G-W	0.75	0.2798	10.2358	735.5085	561.8672
α=1.1	0.80	0.6029	12.6811	889.4878	724.2714
σ=0.9	0.85	1.3588	16.5787	1125.2260	973.0205
ω=1.4	0.90	3.3666	23.7157	1534.9930	1405.2090
λ=0.2	0.95	10.5336	41.1265	2460.9570	2379.0360
	0.99	23.9958	66.0128	3674.0720	3648.2330
	0.70	0.0650	1.9237	29.9475	22.8869
	0.75	0.1169	2.2908	35.0124	28.5501
HT-Gom-W	0.80	0.2172	2.8232	42.1406	36.5356
σ=0.9	0.85	0.4274	3.6613	52.9514	48.6701
ω=1.4	0.90	0.9344	5.1718	71.4883	69.5113
λ=0.2	0.95	2.5877	8.7701	112.3927	115.5431
	0.99	5.5059	13.7747	164.3653	174.0308
	0.70	0.0527	5.3069	307.4204	220.5012
	0.75	0.1172	6.3503	362.3730	278.1300
TIIEHL-W	0.80	0.2665	7.8878	441.1467	360.8052
α=0.9	0.85	0.6376	10.3635	563.6813	489.4927
λ=0.2	0.90	1.6976	14.9726	781.7883	718.582
	0.95	5.8399	26.5446	1294.9170	1256.7160
	0.99	14.2617	43.64812	2001.7400	1995.3450
	0.70	0.1368	6.4427	405.5009	290.2934
	0.75	0.2666	7.6924	476.4526	365.0319
Gom-W	0.80	0.5356	9.5194	577.4105	471.4479
ω=1.4	0.85	1.1383	12.4278	732.8230	635.3274
λ=0.2	0.90	2.6903	17.7504	1005.0430	922.2895
	0.95	8.1132	30.7435	1626.2740	1575.7040
	0.99	18.2247	49.33125	2443.0370	2431.2930
	0.70	0.1301	2.7639	38.7808	29.9105
	0.75	0.2446	3.2797	44.7110	36.8130
TIHT-W	0.80	0.4467	4.0159	52.7810	46.2407
σ=0.9	0.85	0.8455	5.1471	64.4811	59.9561
λ=0.2	0.90	1.7255	7.1093	83.3182	82.0957
	0.95	4.2295	11.4939	121.0701	126.5105
	0.99	8.08503	17.1640	164.3247	177.3807
	0.70	0.0631	1.7858	18.4143	14.6759
	0.75	0.1180	2.1255	21.3896	18.1676
W	0.80	0.2253	2.6155	25.5060	23.0203
λ=0.2	0.85	0.4492	3.3797	31.6019	30.2414
	0.90	0.9753	4.7336	41.6922	42.2566
	0.95	2.5939	7.8567	62.7110	67.4322
	0.99	5.2574	12.0302	87.7154	97.5527

Contd...

TIIEHL-Gom-W	0.70	0.0527	5.3069	307.4204	220.5012
α=1.1	0.75	0.1172	6.3503	362.3730	278.1300
ω=1.4	0.80	0.2665	7.8878	441.1467	360.8052
λ=1.0	0.85	0.6376	10.3635	563.6813	489.4927
	0.90	1.6976	14.9725	781.7883	718.5820
	0.95	5.8399	26.5445	1294.9170	1256.7160
	0.99	14.2617	43.64812	2001.7400	1995.3450
EOWTLL	0.70	0.0024	0.3290	0.5594	0.7206
α=0.08	0.75	0.0070	0.3939	0.6459	0.8784
b=1.7	0.80	0.0193	0.4894	0.7619	1.0989
β=0.4	0.85	0.0523	0.6415	0.9233	1.4263
c=1.2	0.90	0.1477	0.9165	1.1576	1.9583
	0.95	0.5039	1.5504	1.5017	2.9769
	0.99	1.1224	2.3420	1.7191	4.0181
APExLLD	0.70	0.0549	0.2570	1.8175	1.5293
α=0.02	0.75	0.0672	0.2963	2.1693	1.9232
a=1.2	0.80	0.0841	0.3516	2.6919	2.5050
b=0.2	0.85	0.1093	0.4368	3.5506	3.4548
c=0.7	0.90	0.1534	0.5908	5.2287	5.2966
	0.95	0.2632	0.9839	10.0146	10.4977
	0.99	0.9170	3.1527	41.0046	43.7472

5. Special Cases

We introduce several specific cases for the HT-TIIExHL-G-G distribution. These are constructed using baseline distributions such as Weibull, log-logistic, Rayleigh, and Burr III.

5.1 *Heavy-Tailed-Type II Exponentiated Half Logistic-Gompertz-Weibull (HT-TIIExHL-G-W) Distribution*

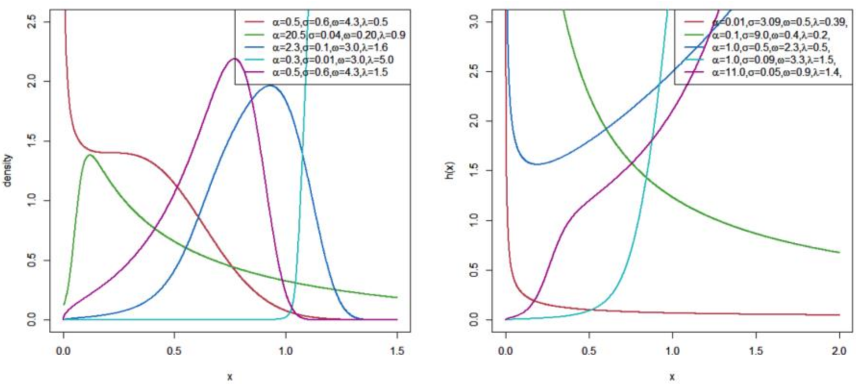

Figure 1
Graphs the pdf and hrf for the HT-TIIExHL-G-W distribution

The shape of the distribution can exhibit different patterns: almost symmetric, right-skewed, or left-skewed as shown Figure 1. Moreover, the hrf displays several shapes including bathtub, decreasing, and increasing.

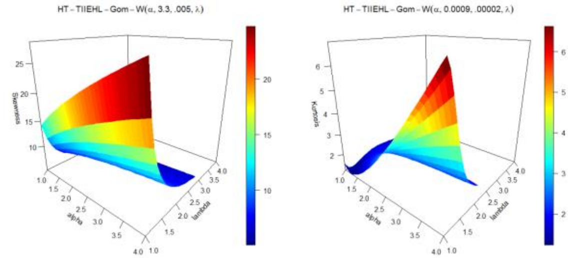

Figure 2
Plots of the skewness and kurtosis for the HT-TIIExHL-G-W distribution

To investigate the impact of the distribution's parameters on its skewness and kurtosis, we held the values of σ and ω fixed while varying the values of α and λ. The resulting plots for the kurtosis and skewness of the HT-TIIExHL-G-W distribution are illustrated in Figure 2. It can be observed that both the kurtosis and skewness of the distribution increase as α and λ increase.

5.2 *Heavy-Tailed-Type II Exponentiated Half Logistic-Gompertz-Log-Logistic (HT-TIIExHL-G-LLoG) Distribution*

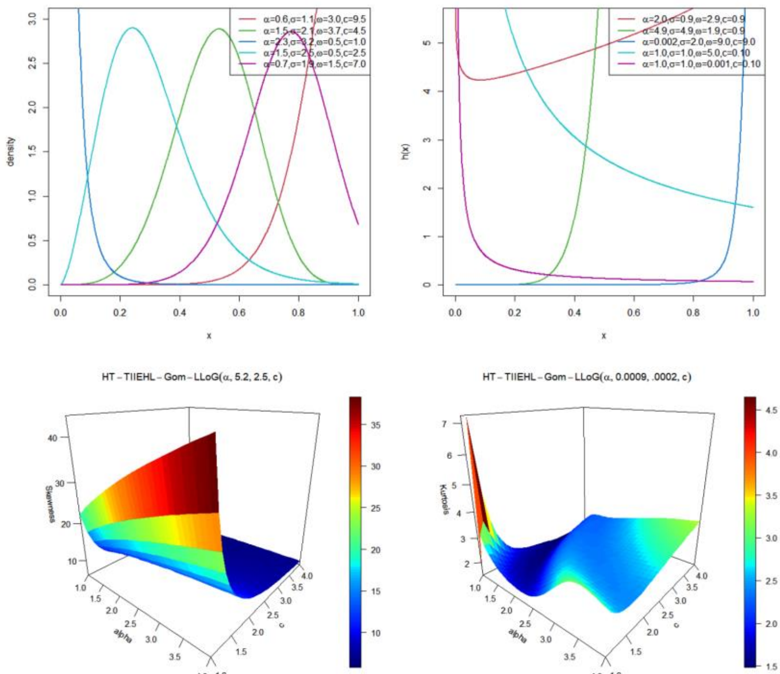

Figure 3
Graphs of the pdf, hrf, skewness and kurtosis for the HT-TIIExHL-G-LLoG distribution

The HT-TIIExHL-G-LLoG distribution's pdf and hrf plots are shown in Figure 3. This distribution can have left-skewed, right-skewed, or nearly symmetrical features, and its hrf can have both monotonic and non-monotonic forms. When we hold σ and ω constant while varying α and c, we present plots depicting the skewness and kurtosis of the HT-TIIExHL-G-LLoG distribution in Figure 3. Figure 3 illustrates that this distribution is versatile, accommodating a wide range of skewness and kurtosis levels when the different parameters are fixed.

5.3 *Heavy-Tailed-Type II Exponentiated Half Logistic-Gompertz-Rayleigh (HT-TIIExHL-G-R) Distribution*

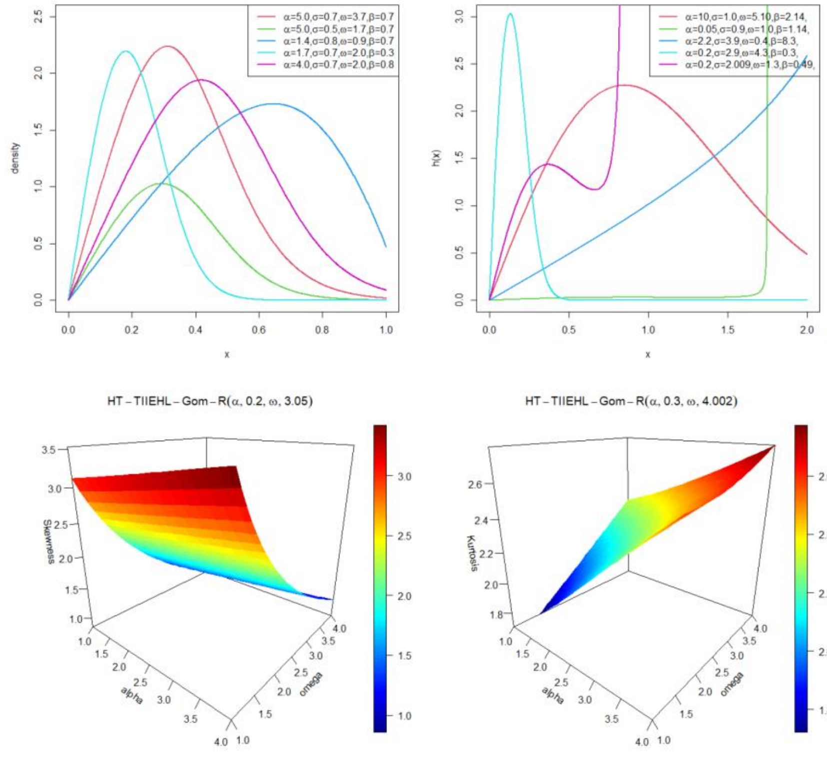

Figure 4
Graphs of the pdf, hrf, skewness and kurtosis for the HT-TIIExHL-Gom-R distribution

Figure 4 displays the pdf and hrf plots for the HT-TIIExHL-G-R distribution. This distribution can exhibit nearly symmetric, right-skewed, or left-skewed characteristics. The hazard rate function displays various shapes, including uni-modal, upside bath-tub, increasing, reverse-J, and upside bath-tub followed by bath-tub shapes. From Figure 4, we can observe that as α and ω

increase, the skewness and kurtosis of the HT-TIIExHL-G-R distribution also increase, while keeping the parameters σ and β constant.

5.4 *Heavy-Tailed-Type II Exponentiated Half Logistic-Gompertz-Burr III (HT-TIIExHL-G-B) Distribution*

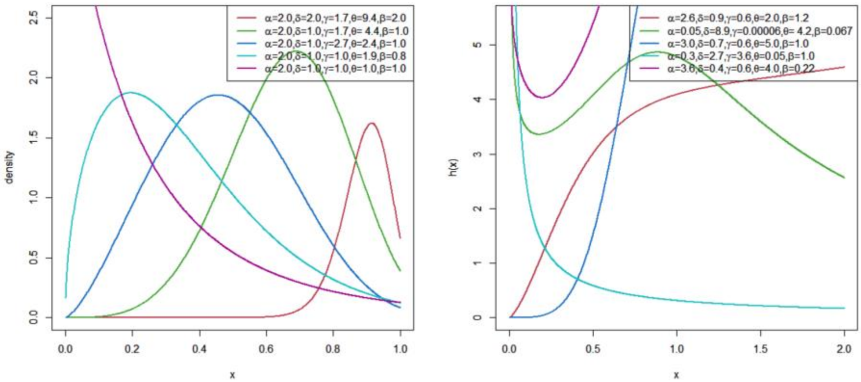

Figure 5
Graphs of the pdf and hrf for the HT-TIIExHL-G-B distribution

We present the pdf and hrf graphs for the HT-TIIExHL-G-B distribution in Figure 5. The distribution's density can accommodate various shapes. The hrf can take both monotonic and non monotonic shapes.

6. Simulation Study

Seven parameter estimation methods for the HT-TIIExHL-G-W distribution was carried out through Monte Carlo simulation study using the R software. The outcomes of these simulations are presented in Tables 2 and 3. Our simulations encompassed N = 3000 independent samples, each drawn from the HT-TIIExHL-G-W distribution, with sample of sizes n = 25, 50, 100, 200, 400, 800, and 1000. To evaluate the performance of the estimated parameters, denoted as $\widehat{\Theta}$, we employed the average bias (AvBias) and root mean square error (RMSe) metrics. These measures were computed using the following formulas:

$$ABias(\widehat{\Theta}) = \frac{\sum_{i=1}^{N} \widehat{\Theta}_i}{N} - \Theta, RMSE(\widehat{\Theta}) = \sqrt{\frac{\sum_{i=1}^{N} (\widehat{\Theta}_i - \Theta)^2}{N}},$$

where Θ represents the true parameter value.

Tables 2 and 3 contain information about the sum of ranks ($\sum ranks$), which represents the cumulative ranks. Within each metric and among all estimators, the subscript denotes the rank assigned. For instance, in Table 1, the RMSe of the estimated parameter α using the LS method is reported as $2.1996_{(4)}$ for the sample size n = 25. This signifies that among all estimators, the LS method achieved the fourth-best RMSe ranking for the parameter α when n =

25. In summary, for a sample size of 25, the LS method demonstrated the fourth lowest RMSe for estimating the parameter α compared to all other estimators. Table 4 displays the rankings of all the methods used for estimation for the HT-TIIExHL-G-W distribution, based on several values of the model parameters. The rankings are given for both the partial and overall performance of the methods.

Consequently, from an examination of the results presented in Tables 2 and 3, it becomes apparent that as the sample size increases, both the RMSe and AvBias decrease steadily for all parameters. This compelling evidence demonstrates that the HT-TIIExHL-G-W distribution consistently generates reliable parameter estimates. Furthermore, it reinforces the notion that larger sample sizes contribute to enhanced precision in parameter estimation.

Figures 6 and 7 reveal how the RMSe values for parameter estimates consistently reduced with larger sample sizes, regardless of the estimation techniques employed. From the Table 4, it is evident that the MLE method yielded better parameter estimates for the HT-TIIExHL-G-W distribution, securing the top rank. Following MLE, the AD method ranked second, and then, WLS method ranked the third position. Notably, the LS method exhibited least performance, ranking the lowest among the estimation techniques.

Table 2
Results of Simulations using Different Estimation Techniques
for $\alpha = 1.0, \sigma = 0.5, \omega = 1.5, \lambda = 1.0$

		LS		CVM		AD		WLS		RADE		MPS		MLE	
parameter	n	RMSe	AvBIAS	RMSe	AvBIAS	RMSe	AvBIAS	RMSe	AvBIAS	RMSe	AvBIAS	RMSe	AvBIAS	RMSe	AvBIAS
α	25	2.1996$_{(4)}$	0.1212$_{(2)}$	2.4963$_{(6)}$	0.2822$_{(5)}$	2.0694$_{(3)}$	-0.0497$_{(1)}$	1.7162$_{(2)}$	-0.1916$_{(3)}$	2.3197$_{(5)}$	0.2744$_{(4)}$	7.2546$_{(7)}$	0.5634$_{(7)}$	1.6318$_{(1)}$	-0.3122$_{(6)}$
σ	25	0.5547$_{(2)}$	0.2586$_{(2)}$	0.6087$_{(5)}$	0.3289$_{(5)}$	0.5813$_{(4)}$	0.3102$_{(4)}$	0.5770$_{(3)}$	0.2856$_{(1)}$	0.5540$_{(1)}$	0.3046$_{(3)}$	0.8165$_{(7)}$	0.6403$_{(7)}$	0.6543$_{(6)}$	0.4705$_{(6)}$
ω	25	1.6129$_{(5)}$	0.7253$_{(6)}$	1.4324$_{(4)}$	0.4645$_{(4)}$	1.6380$_{(6)}$	0.7063$_{(5)}$	1.7901$_{(7)}$	0.9445$_{(7)}$	1.3714$_{(3)}$	0.3916$_{(3)}$	0.9178$_{(1)}$	-0.0516$_{(1)}$	1.1223$_{(2)}$	0.3545$_{(2)}$
λ	25	0.4929$_{(4)}$	-0.0677$_{(2)}$	0.4920$_{(3)}$	0.0735$_{(3)}$	0.5281$_{(5)}$	0.0112$_{(1)}$	1.7901$_{(7)}$	-0.0995$_{(4)}$	0.4800$_{(2)}$	0.1006$_{(5)}$	0.7505$_{(6)}$	0.5239$_{(7)}$	0.4753$_{(1)}$	0.1696$_{(6)}$
$\sum ranks$		26		35		29		34		26		43		30	
α	50	1.3418$_{(5)}$	-0.1357$_{(3)}$	1.6630$_{(7)}$	0.0097$_{(1)}$	0.9662$_{(4)}$	-0.2793$_{(4)}$	0.9387$_{(3)}$	-0.3453$_{(6)}$	1.3467$_{(6)}$	-0.1003$_{(2)}$	0.9078$_{(2)}$	-0.4103$_{(7)}$	0.8410$_{(1)}$	-0.2951$_{(5)}$
σ	50	0.5048$_{(2)}$	0.2462$_{(1)}$	0.5535$_{(5)}$	0.2894$_{(4)}$	0.5349$_{(4)}$	0.2857$_{(3)}$	0.4994$_{(1)}$	0.2526$_{(2)}$	0.5187$_{(3)}$	0.2936$_{(5)}$	0.7256$_{(1)}$	0.5741$_{(7)}$	0.6082$_{(6)}$	0.3859$_{(6)}$
ω	50	1.4754$_{(6)}$	0.7090$_{(6)}$	1.3472$_{(4)}$	0.4820$_{(4)}$	1.4169$_{(5)}$	0.6578$_{(5)}$	1.5340$_{(7)}$	0.8087$_{(7)}$	1.3072$_{(3)}$	0.4503$_{(3)}$	0.8134$_{(1)}$	0.0736$_{(1)}$	1.0184$_{(2)}$	0.2750$_{(2)}$
λ	50	0.4350$_{(3)}$	-0.0769$_{(4)}$	0.4490$_{(4)}$	0.0351$_{(2)}$	0.4508$_{(5)}$	-0.0255$_{(1)}$	0.4538$_{(6)}$	-0.0831$_{(5)}$	0.4307$_{(2)}$	0.0476$_{(3)}$	0.5070$_{(7)}$	0.3093$_{(7)}$	0.4015$_{(1)}$	0.1171$_{(6)}$
$\sum ranks$		30		31		31		31		37		33		29	
α	100	0.8977$_{(7)}$	-0.2977$_{(6)}$	0.8391$_{(5)}$	-0.2976$_{(5)}$	0.7288$_{(2)}$	-0.2350$_{(2)}$	0.7290$_{(3)}$	-0.2893$_{(4)}$	0.8744$_{(6)}$	-0.2788$_{(3)}$	0.7134$_{(1)}$	-0.3769$_{(7)}$	0.8289$_{(4)}$	-0.1998$_{(1)}$
σ	100	0.4743$_{(3)}$	0.2296$_{(3)}$	0.5076$_{(5)}$	0.2775$_{(6)}$	0.4520$_{(2)}$	0.2030$_{(2)}$	0.4416$_{(1)}$	0.1990$_{(1)}$	0.4816$_{(4)}$	0.2547$_{(4)}$	0.6332$_{(7)}$	0.4615$_{(7)}$	0.5220$_{(6)}$	0.2717$_{(5)}$
ω	100	1.3302$_{(7)}$	0.7115$_{(7)}$	1.2060$_{(4)}$	0.5669$_{(5)}$	1.1311$_{(3)}$	0.5253$_{(4)}$	1.2562$_{(6)}$	0.6390$_{(6)}$	1.2289$_{(5)}$	0.5074$_{(3)}$	0.6819$_{(1)}$	0.0616$_{(1)}$	0.8926$_{(2)}$	0.3067$_{(2)}$
λ	100	0.3871$_{(6)}$	-0.0918$_{(6)}$	0.3858$_{(5)}$	-0.0241$_{(2)}$	0.3625$_{(2)}$	-0.0442$_{(4)}$	0.3690$_{(3)}$	-0.0812$_{(5)}$	0.4050$_{(7)}$	-0.0003$_{(1)}$	0.3776$_{(4)}$	0.2097$_{(7)}$	0.3319$_{(1)}$	0.0395$_{(3)}$
$\sum ranks$		43		37		21		29		33		35		24	
α	200	0.6294$_{(7)}$	-0.2964$_{(4)}$	0.6247$_{(5)}$	-0.3042$_{(7)}$	0.5486$_{(2)}$	-0.2024$_{(2)}$	0.5303$_{(1)}$	-0.2193$_{(3)}$	0.6266$_{(6)}$	-0.2996$_{(6)}$	0.6042$_{(4)}$	-0.2971$_{(5)}$	0.5680$_{(3)}$	-0.1865$_{(1)}$
σ	200	0.4173$_{(3)}$	0.1808$_{(3)}$	0.4399$_{(6)}$	0.2094$_{(6)}$	0.3709$_{(1)}$	0.1401$_{(1)}$	0.3763$_{(2)}$	0.1454$_{(2)}$	0.4208$_{(4)}$	0.2092$_{(2)}$	0.5528$_{(7)}$	0.3556$_{(7)}$	0.4222$_{(5)}$	0.2021$_{(4)}$
ω	200	1.0951$_{(7)}$	0.5846$_{(7)}$	1.0510$_{(5)}$	0.5155$_{(6)}$	0.8944$_{(4)}$	0.4039$_{(4)}$	0.8512$_{(3)}$	0.3878$_{(3)}$	1.0698$_{(6)}$	0.4361$_{(5)}$	0.5338$_{(1)}$	0.0640$_{(1)}$	0.6496$_{(2)}$	0.1989$_{(2)}$
λ	200	0.3297$_{(6)}$	-0.0862$_{(6)}$	0.3238$_{(5)}$	-0.0553$_{(5)}$	0.2874$_{(3)}$	-0.0492$_{(4)}$	0.2900$_{(4)}$	-0.0436$_{(3)}$	0.3552$_{(7)}$	-0.0136$_{(1)}$	0.2756$_{(2)}$	0.1330$_{(7)}$	0.2427$_{(1)}$	0.0279$_{(2)}$
$\sum ranks$		43		45		21		21		37		34		20	
α	400	0.4877$_{(7)}$	-0.2041$_{(5)}$	0.4811$_{(6)}$	-0.2146$_{(6)}$	0.4196$_{(3)}$	-0.1169$_{(1)}$	0.3979$_{(1)}$	-0.1449$_{(3)}$	0.4682$_{(5)}$	-0.2334$_{(7)}$	0.4594$_{(4)}$	-0.1913$_{(4)}$	0.4137$_{(2)}$	-0.1277$_{(2)}$
σ	400	0.3319$_{(4)}$	0.1089$_{(3)}$	0.3392$_{(5)}$	-0.2146$_{(6)}$	0.2764$_{(2)}$	0.0775$_{(1)}$	0.2683$_{(1)}$	0.0849$_{(2)}$	0.3453$_{(6)}$	0.1439$_{(5)}$	0.4081$_{(7)}$	0.2158$_{(7)}$	0.3210$_{(3)}$	0.1299$_{(4)}$
ω	400	0.8306$_{(7)}$	0.4139$_{(7)}$	0.8212$_{(6)}$	0.4015$_{(6)}$	0.6043$_{(4)}$	0.2479$_{(4)}$	0.5961$_{(3)}$	0.2374$_{(3)}$	0.8055$_{(5)}$	0.3076$_{(5)}$	0.3894$_{(1)}$	0.0224$_{(1)}$	0.4198$_{(2)}$	0.0915$_{(2)}$
λ	400	0.2704$_{(6)}$	-0.0725$_{(6)}$	0.2690$_{(5)}$	-0.0582$_{(5)}$	0.2069$_{(3)}$	-0.0396$_{(4)}$	0.2132$_{(4)}$	-0.0311$_{(3)}$	0.2886$_{(7)}$	-0.0172$_{(1)}$	0.1985$_{(2)}$	0.0853$_{(7)}$	0.1810$_{(1)}$	0.0235$_{(2)}$
$\sum ranks$		45		45		22		20		41		33		18	
α	800	0.3536$_{(6)}$	-0.1285$_{(6)}$	0.3580$_{(7)}$	-0.1115$_{(4)}$	0.2994$_{(2)}$	-0.0538$_{(1)}$	0.2766$_{(1)}$	-0.0721$_{(2)}$	0.3376$_{(5)}$	-0.1326$_{(7)}$	0.3269$_{(4)}$	-0.1224$_{(5)}$	0.3033$_{(3)}$	-0.0725$_{(3)}$
σ	800	0.2525$_{(6)}$	0.0614$_{(4)}$	0.2465$_{(5)}$	0.0585$_{(3)}$	0.1729$_{(1)}$	0.0309$_{(1)}$	0.1837$_{(2)}$	0.0417$_{(2)}$	0.2276$_{(4)}$	0.0626$_{(5)}$	0.2565$_{(7)}$	0.1108$_{(7)}$	0.2111$_{(3)}$	0.0663$_{(6)}$
ω	800	0.5905$_{(6)}$	0.2521$_{(7)}$	0.5494$_{(5)}$	0.2336$_{(6)}$	0.3662$_{(3)}$	0.1285$_{(4)}$	0.3711$_{(4)}$	0.1104$_{(3)}$	0.5979$_{(7)}$	0.2067$_{(5)}$	0.2757$_{(1)}$	0.0106$_{(1)}$	0.3023$_{(2)}$	0.0503$_{(2)}$
λ	800	0.2192$_{(6)}$	-0.0460$_{(6)}$	0.2051$_{(5)}$	-0.0410$_{(5)}$	0.1476$_{(3)}$	-0.0248$_{(3)}$	0.1544$_{(4)}$	-0.0144$_{(2)}$	0.2289$_{(7)}$	-0.0250$_{(4)}$	0.1342$_{(2)}$	0.0466$_{(7)}$	0.1324$_{(1)}$	0.0104$_{(1)}$
$\sum ranks$		47		40		18		20		44		34		21	
α	1000	0.3091$_{(6)}$	-0.1213$_{(7)}$	0.3114$_{(7)}$	-0.1056$_{(5)}$	0.2667$_{(3)}$	-0.0316$_{(1)}$	0.2581$_{(1)}$	-0.0728$_{(3)}$	0.2885$_{(5)}$	-0.1158$_{(6)}$	0.2841$_{(4)}$	-0.1020$_{(4)}$	0.2637$_{(2)}$	-0.0558$_{(2)}$
σ	1000	0.2055$_{(5)}$	0.0516$_{(5)}$	0.2294$_{(7)}$	0.0602$_{(6)}$	0.1538$_{(1)}$	0.0269$_{(1)}$	0.1691$_{(2)}$	0.0436$_{(2)}$	0.1963$_{(4)}$	0.0459$_{(3)}$	0.2164$_{(6)}$	0.0912$_{(7)}$	0.1759$_{(3)}$	0.0490$_{(4)}$
ω	1000	0.5176$_{(6)}$	0.2010$_{(7)}$	0.4720$_{(5)}$	0.1572$_{(5)}$	0.3257$_{(4)}$	0.0696$_{(3)}$	0.3115$_{(3)}$	0.0841$_{(4)}$	0.5516$_{(7)}$	0.1835$_{(6)}$	0.2445$_{(1)}$	-0.0167$_{(1)}$	0.2554$_{(2)}$	0.0350$_{(2)}$
λ	1000	0.1949$_{(6)}$	-0.0329$_{(6)}$	0.1893$_{(5)}$	-0.0183$_{(4)}$	0.1375$_{(4)}$	-0.0052$_{(2)}$	0.1342$_{(3)}$	-0.0050$_{(1)}$	0.2148$_{(7)}$	-0.0258$_{(5)}$	0.1251$_{(2)}$	0.0503$_{(7)}$	0.1190$_{(1)}$	0.0089$_{(3)}$
$\sum ranks$		48		44		19		19		43		31		19	

Table 3
Results of Simulations using Different Estimation Techniques
$\alpha = 1.0, \sigma = 0.8, \omega = 1.0, \lambda = 2.0$

		LS		CVM		AD		WLS		RADE		MPS		MLE	
parameter	n	RMSe	AvBIAS	RMSe	AvBIAS	RMSe	AvBIAS	RMSe	AvBIAS	RMSe	AvBIAS	RMSe	AvBIAS	RMSe	AvBIAS
α	25	1.4288$_{(6)}$	-0.1335$_{(3)}$	1.3737$_{(5)}$	-0.1581$_{(5)}$	1.1942$_{(3)}$	-0.1130$_{(2)}$	1.2082$_{(4)}$	-0.1568$_{(4)}$	1.6582$_{(7)}$	0.0315$_{(1)}$	0.8378$_{(2)}$	-0.4563$_{(4)}$	0.8241$_{(1)}$	-0.4112$_{(6)}$
σ	25	0.8047$_{(6)}$	0.3260$_{(3)}$	0.8162$_{(7)}$	0.3777$_{(5)}$	0.7663$_{(4)}$	0.2943$_{(2)}$	0.8022$_{(5)}$	0.2905$_{(1)}$	0.7626$_{(3)}$	0.3464$_{(4)}$	0.7448$_{(2)}$	0.6031$_{(7)}$	0.6453$_{(1)}$	0.4493$_{(6)}$
ω	25	1.7218$_{(6)}$	0.7945$_{(6)}$	1.6582$_{(4)}$	0.7393$_{(4)}$	1.6687$_{(5)}$	0.7498$_{(5)}$	1.8293$_{(7)}$	0.8530$_{(7)}$	1.3906$_{(3)}$	0.5236$_{(2)}$	0.9987$_{(1)}$	0.4703$_{(1)}$	1.0965$_{(2)}$	0.6000$_{(3)}$
λ	25	0.8727$_{(6)}$	-0.3122$_{(6)}$	0.8634$_{(5)}$	-0.1269$_{(3)}$	0.8422$_{(4)}$	-0.1708$_{(4)}$	0.9018$_{(7)}$	-0.2938$_{(5)}$	0.7906$_{(2)}$	-0.0400$_{(2)}$	0.7970$_{(3)}$	0.4158$_{(7)}$	0.6266$_{(1)}$	0.0295$_{(1)}$
$\sum ranks$		42		38		29		40		24		27		21	
α	50	1.0257$_{(5)}$	-0.1715$_{(4)}$	0.9835$_{(3)}$	-0.2079$_{(5)}$	1.1272$_{(7)}$	0.0233$_{(2)}$	1.0799$_{(6)}$	0.0027$_{(1)}$	1.0128$_{(4)}$	-0.1298$_{(1)}$	0.7811$_{(1)}$	-0.4162$_{(7)}$	0.8314$_{(2)}$	-0.2461$_{(6)}$
σ	50	0.7064$_{(6)}$	0.2706$_{(3)}$	0.7088$_{(7)}$	0.3396$_{(5)}$	0.6265$_{(1)}$	0.2000$_{(2)}$	0.6345$_{(2)}$	0.1742$_{(1)}$	0.6483$_{(4)}$	0.2964$_{(4)}$	0.7049$_{(5)}$	0.5430$_{(7)}$	0.6443$_{(3)}$	0.3965$_{(6)}$
ω	50	1.5395$_{(7)}$	0.7142$_{(7)}$	1.3636$_{(5)}$	0.5899$_{(5)}$	1.3175$_{(4)}$	0.5632$_{(4)}$	1.3930$_{(6)}$	0.6179$_{(6)}$	1.2735$_{(3)}$	0.5106$_{(3)}$	0.7979$_{(1)}$	0.3737$_{(2)}$	0.8358$_{(2)}$	0.3636$_{(1)}$
λ	50	0.7756$_{(7)}$	-0.2658$_{(7)}$	0.7060$_{(5)}$	-0.1307$_{(3)}$	0.6825$_{(3)}$	-0.1777$_{(4)}$	0.7267$_{(6)}$	-0.2336$_{(6)}$	0.7043$_{(4)}$	-0.1053$_{(2)}$	0.5922$_{(2)}$	0.2239$_{(5)}$	0.5225$_{(1)}$	0.0274$_{(1)}$
$\sum ranks$		46		37		27		34		29		30		22	
α	100	0.9725$_{(6)}$	-0.0315$_{(1)}$	0.9240$_{(4)}$	-0.0865$_{(3)}$	0.9822$_{(7)}$	0.1134$_{(5)}$	0.9710$_{(5)}$	0.0924$_{(4)}$	0.8735$_{(3)}$	-0.0601$_{(2)}$	0.7458$_{(1)}$	-0.3649$_{(7)}$	0.8258$_{(2)}$	-0.1160$_{(6)}$
σ	100	0.5874$_{(4)}$	0.1793$_{(3)}$	0.5962$_{(5)}$	0.2252$_{(5)}$	0.5641$_{(2)}$	0.1277$_{(2)}$	0.5494$_{(1)}$	0.1149$_{(1)}$	0.5734$_{(3)}$	0.1985$_{(4)}$	0.6506$_{(7)}$	0.4845$_{(7)}$	0.6029$_{(6)}$	0.2986$_{(6)}$
ω	100	1.1858$_{(7)}$	0.5544$_{(7)}$	1.0784$_{(5)}$	0.5176$_{(6)}$	0.9026$_{(3)}$	0.4021$_{(3)}$	1.0068$_{(4)}$	0.4750$_{(5)}$	1.0977$_{(6)}$	0.4595$_{(4)}$	0.5900$_{(1)}$	0.3022$_{(1)}$	0.6860$_{(2)}$	0.3096$_{(2)}$
λ	100	0.6272$_{(7)}$	-0.2367$_{(7)}$	0.5860$_{(5)}$	-0.1924$_{(5)}$	0.5389$_{(3)}$	-0.1797$_{(4)}$	0.5810$_{(4)}$	-0.2280$_{(6)}$	0.6080$_{(6)}$	-0.1408$_{(2)}$	0.4206$_{(1)}$	0.1435$_{(3)}$	0.4575$_{(2)}$	-0.0212$_{(1)}$
$\sum ranks$		42		38		29		30		30		28		27	
α	200	0.8910$_{(7)}$	0.0479$_{(4)}$	0.8210$_{(5)}$	-0.0383$_{(3)}$	0.8469$_{(6)}$	0.0806$_{(5)}$	0.7789$_{(4)}$	0.0223$_{(1)}$	0.7487$_{(3)}$	-0.0324$_{(2)}$	0.7062$_{(1)}$	-0.3090$_{(7)}$	0.7208$_{(2)}$	-0.1019$_{(6)}$
σ	200	0.5448$_{(5)}$	0.1332$_{(3)}$	0.5467$_{(6)}$	0.1771$_{(5)}$	0.5075$_{(2)}$	0.1164$_{(1)}$	0.4959$_{(1)}$	0.1274$_{(2)}$	0.5235$_{(3)}$	0.1534$_{(4)}$	0.6226$_{(7)}$	0.4306$_{(7)}$	0.5397$_{(4)}$	0.2495$_{(6)}$
ω	200	0.8627$_{(6)}$	0.4260$_{(6)}$	0.8751$_{(7)}$	0.4271$_{(7)}$	0.6592$_{(3)}$	0.3098$_{(3)}$	0.6846$_{(4)}$	0.3391$_{(4)}$	0.7885$_{(5)}$	0.3801$_{(5)}$	0.4290$_{(1)}$	0.2248$_{(1)}$	0.5121$_{(2)}$	0.2353$_{(1)}$
λ	200	0.5160$_{(7)}$	-0.2225$_{(7)}$	0.4932$_{(6)}$	-0.1719$_{(6)}$	0.4332$_{(3)}$	-0.1480$_{(3)}$	0.4379$_{(4)}$	-0.1583$_{(4)}$	0.4777$_{(5)}$	-0.1651$_{(5)}$	0.3221$_{(1)}$	0.0871$_{(2)}$	0.3446$_{(2)}$	-0.0281$_{(1)}$
$\sum ranks$		45		45		26		24		32		27		24	
α	400	0.7942$_{(6)}$	0.0858$_{(4)}$	0.8000$_{(7)}$	0.0596$_{(3)}$	0.7526$_{(5)}$	0.1095$_{(6)}$	0.6604$_{(3)}$	0.0387$_{(2)}$	0.6761$_{(4)}$	0.0125$_{(1)}$	0.6050$_{(1)}$	-0.2802$_{(7)}$	0.6291$_{(2)}$	-0.0866$_{(5)}$
σ	400	0.4817$_{(4)}$	0.1016$_{(3)}$	0.4984$_{(6)}$	0.1268$_{(5)}$	0.4419$_{(2)}$	0.0852$_{(1)}$	0.4186$_{(1)}$	0.0977$_{(2)}$	0.4781$_{(3)}$	0.1204$_{(4)}$	0.5659$_{(7)}$	0.3712$_{(7)}$	0.4958$_{(5)}$	0.2159$_{(6)}$
ω	400	0.5956$_{(7)}$	0.2925$_{(7)}$	0.5615$_{(5)}$	0.2900$_{(6)}$	0.4021$_{(4)}$	0.1938$_{(3)}$	0.3908$_{(3)}$	0.1951$_{(4)}$	0.5654$_{(6)}$	0.2683$_{(5)}$	0.3346$_{(1)}$	0.1721$_{(2)}$	0.3465$_{(2)}$	0.1583$_{(1)}$
λ	400	0.3873$_{(6)}$	-0.1598$_{(7)}$	0.3833$_{(5)}$	-0.1425$_{(6)}$	0.3120$_{(4)}$	-0.1076$_{(4)}$	0.2980$_{(3)}$	-0.1001$_{(3)}$	0.3943$_{(7)}$	-0.1241$_{(5)}$	0.2450$_{(1)}$	0.0652$_{(2)}$	0.2576$_{(2)}$	-0.0189$_{(1)}$
$\sum ranks$		44		43		28		21		35		28		24	
α	800	0.6396$_{(6)}$	0.0423$_{(5)}$	0.6527$_{(7)}$	0.0307$_{(3)}$	0.5360$_{(5)}$	-0.0129$_{(2)}$	0.4899$_{(1)}$	0.0035$_{(1)}$	0.5240$_{(4)}$	-0.0321$_{(4)}$	0.5229$_{(3)}$	-0.2468$_{(7)}$	0.5087$_{(2)}$	-0.0740$_{(6)}$
σ	800	0.4218$_{(4)}$	0.0923$_{(2)}$	0.4326$_{(6)}$	0.1115$_{(4)}$	0.3951$_{(2)}$	0.1139$_{(5)}$	0.3406$_{(1)}$	0.0789$_{(1)}$	0.4128$_{(3)}$	0.1112$_{(3)}$	0.5074$_{(7)}$	0.3073$_{(7)}$	0.4229$_{(5)}$	0.1616$_{(6)}$
ω	800	0.3714$_{(6)}$	0.2064$_{(7)}$	0.3530$_{(5)}$	0.1843$_{(5)}$	0.2660$_{(4)}$	0.1267$_{(3)}$	0.2509$_{(1)}$	0.1120$_{(1)}$	0.3796$_{(7)}$	0.1857$_{(6)}$	0.2651$_{(3)}$	0.1355$_{(4)}$	0.2546$_{(2)}$	0.1137$_{(2)}$
λ	800	0.3000$_{(7)}$	-0.1173$_{(7)}$	0.2815$_{(5)}$	-0.0907$_{(6)}$	0.2186$_{(4)}$	-0.0519$_{(4)}$	0.1967$_{(3)}$	-0.0483$_{(3)}$	0.2914$_{(6)}$	-0.0858$_{(5)}$	0.1766$_{(1)}$	0.0425$_{(2)}$	0.1940$_{(2)}$	-0.0177$_{(1)}$
$\sum ranks$		44		43		29		12		38		34		26	
α	1000	0.6171$_{(6)}$	0.0499$_{(5)}$	0.6490$_{(7)}$	0.0553$_{(6)}$	0.4893$_{(3)}$	0.0283$_{(3)}$	0.4910$_{(4)}$	0.0024$_{(1)}$	0.5070$_{(5)}$	-0.0079$_{(2)}$	0.4848$_{(2)}$	-0.2034$_{(7)}$	0.4589$_{(1)}$	-0.0461$_{(4)}$
σ	1000	0.4059$_{(5)}$	0.0870$_{(3)}$	0.4096$_{(6)}$	0.0922$_{(4)}$	0.3349$_{(2)}$	0.0656$_{(1)}$	0.3337$_{(1)}$	0.0689$_{(2)}$	0.3854$_{(4)}$	0.0943$_{(5)}$	0.4610$_{(7)}$	0.2541$_{(7)}$	0.3658$_{(3)}$	0.1189$_{(6)}$
ω	1000	0.3121$_{(6)}$	0.1653$_{(6)}$	0.3188$_{(7)}$	0.1731$_{(7)}$	0.2341$_{(4)}$	0.0941$_{(3)}$	0.2263$_{(2)}$	0.0935$_{(2)}$	0.3024$_{(5)}$	0.1448$_{(5)}$	0.2327$_{(3)}$	0.1160$_{(4)}$	0.2176$_{(1)}$	0.0865$_{(1)}$
λ	1000	0.2572$_{(6)}$	-0.0967$_{(7)}$	0.2567$_{(5)}$	-0.0917$_{(6)}$	0.1919$_{(4)}$	-0.0489$_{(4)}$	0.1879$_{(3)}$	-0.0463$_{(3)}$	0.2617$_{(7)}$	-0.0690$_{(5)}$	0.1626$_{(1)}$	0.0315$_{(2)}$	0.1723$_{(2)}$	-0.0147$_{(1)}$
$\sum ranks$		44		48		24		18		38		33		19	

Table 4
Partial and Overall Rankings of Estimation Techniques for the HT-TIIExHL-G-W Distribution

Parameters	n	LS	CVM	AD	WLS	RAD	MPS	MLE
$\alpha = 1.0$, $\sigma = 0.5$, $\omega = 1.5$, $\lambda = 1.0$	25	1.5	6	3	5	1.5	7	4
	50	2	4	4	4	7	6	1
	100	7	6	1	3	4	5	2
	200	6	7	2.5	2.5	5	4	1
	400	6.5	6.5	3	2	5	4	1
	800	7	5	1	2	6	4	3
	1000	7	6	2	2	5	4	2
	25	7	5	4	6	2	3	1
	50	7	6	2	5	3	4	1
	100	7	6	3	4.5	4.5	2	1
$\alpha = 1.0$, $\sigma = 0.8$, $\omega = 1.0$, $\lambda = 2.0$	200	6.5	6.5	3	1.5	5	4	1.5
	400	7	6	3.5	1	5	3.5	2
	800	7	6	3	1	5	4	2
	1000	6	7	3	1	5	4	2
$\sum ranks$		84.5	83	38	40.5	63	58.5	24.5
Overall rank		7	6	2	3	5	4	1

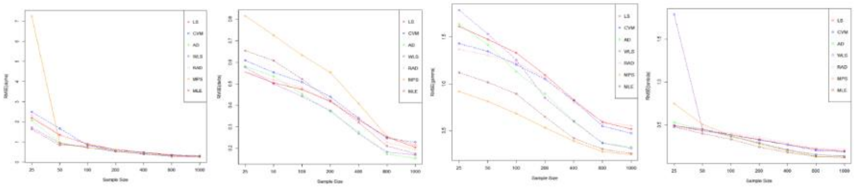

Figure 6
Graphs displaying RMSe in Table 1

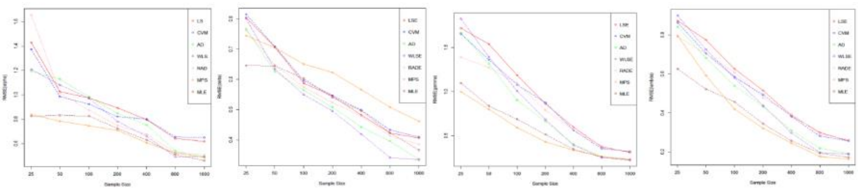

Figure 7
Graphs displaying RMSe in Table 7

7. Applications

We have used three real data examples from medical sciences and engineering to assess the usefulness of the HT-TIIExHL-G-W distribution. We presented several selection criteria goodness-of-fit statistics (GoFs), such as Bayesian Information Criterion (BIC), Akaike Information Criterion (AIC), Consistent Akaike Information Criterion (AICC), and negative 2 log-likelihood (-2 log (L)). We also included other GoFs, as stated by Chen and Balakrishnan [4], specifically Andersen-Darling and Cramér-von Mises.

These statistics serve the purpose of evaluating the goodness-of-fit of different models to the provided dataset. Smaller these statistics' values indicate a better fit of the distribution. Moreover, the Kolmogorov-Smirnov (K-S) statistic and its corresponding p-value were employed to further assess goodness-of-fit. The distribution having smallest K-S value additionally the highest p-value for the K-S statistic is considered to be most suitable fit for the data.

In our analysis, we have included a graphical representation of the HT-TIIExHL-G-W distribution, including fitted density, probability plots, estimated cumulative distribution function (CDF), Kaplan-Meier (K-M) plots, estimated hazard rate function (HRF) plots, profile log-likelihood plots, and total time on test (TTT) plots. The plots are displayed in Figures 10, 11, 12, 13, 17 and 18 correspondingly, among the three sets of data. The figures show that the HT-TIIExHL-G-W distribution fits all data sets adequately.

We employed the R nlm function to perform parameter estimation for the models. The resulting estimated parameters, with their respective standard errors, and the GoFs can be found in Tables 7.1, 7.2, and 7.3. We conducted a comparative analysis of the HT-TIIExHL-G-W model against several other non-nested models. The competing models' names and pdfs are in the appendix.

7.1 *Europe COVID-19 Data*

The initial data set displays the count of COVID-19-related fatalities that occurred in Europe between March 1, 2022, and March 30, 2022. This data is available on the World Health Organization website (https://covid19.who.int/). (Visit the appendix for the observations). The estimated variance-covariance matrix is

$$\begin{bmatrix} 0.0001 & -0.0040 & 0.0002 & -0.0003 \\ -0.0040 & 0.2976 & 0.0016 & -0.0039 \\ 0.0001 & 0.0016 & 0.0001 & -0.0009 \\ -0.0003 & -0.0039 & -0.0009 & 0.0078 \end{bmatrix},$$

and the model parameters' 95% confidence intervals are $\alpha \in [0.0094 \pm 0.0173]$, $\sigma \in [1.2141 \pm 1.0691]$, $\omega \in [0.0094 \pm 0.0226]$ and $\lambda \in [0.6082 \pm 0.1732]$, respectively.

Table 5
MLE's and GoFs for several distributions fitted for Europe Covid-19 data

	Estimates				Statistics							
Model	α	σ	ω	λ	$-2\log L$	AIC	$AICC$	BIC	W^*	A^*	$K-S$	$P-value$
HT-TIIExHL-G-W	0.0094	1.2141	0.0094	0.6081	472.1	480.1	481.6	485.8	0.0499	0.4958	0.1296	0.6283
	(0.0088)	(0.5455)	(0.0015)	(0.0883)								
	b	σ	λ	ω								
TLMOW	0.4453	2.8458	0.0002	1.1454	472.7	480.7	481.2	485.4	0.0879	0.5643	0.1549	0.4052
	(0.0724)	(0.0019)	(6.0423×10^{-5})	(0.0337)								
	ω	b	λ									
TLGW	2.3705×10^{-10}	4.2536	0.0853		557.4	563.4	564.3	567.7	0.0655	0.4789	0.6778	1.266×10^{-14}
	(0.0032)	(0.7753)	(0.0106)									
	a	b	α	θ								
TLWx	0.1686	0.0065	1.0284	0.5853	483.3	491.3	492.9	497.1	0.0744	0.5356	0.1727	0.2798
	(0.0455)	(0.0079)	(0.2892)	(0.1853)								
	b	β	σ	c								
EHL-OWTL-L	1.5932	0.1745	2.0773	0.4738	508.0	516.0	517.5	521.7	0.0623	0.5165	0.3983	0.5808
	(0.9733)	(0.0581)	(0.4009)	(0.1269)								
	α	ω	β									
HTBPTW	0.0781	1.5002	3.5472×10^{-5}		525.2	531.1	532.0	535.5	0.0656	0.4794	0.4669	1.026×10^{-6}
	(0.0127)	(0.2382)	(0.0001)									
	α	b	β	c								
EOWTLL	8.7876	2.8524	0.0524	1.8056	480.8	488.8	490.3	494.5	0.0664	0.4851	0.1801	0.2367
	(1.8830)	(2.7021)	(0.0240)	(0.7807)								

The MLEs and GoFs of the models for covid-19 data from Europe are displayed in Table 5. Table 5 clearly displays that the HT-TIIExHL-G-W has a better fit to the data when compared to the competing models considered in this work because it has the lower GoFs values and a higher K-S p-value. The maximum likelihood estimates are shown by the graphs of the profile log-likelihood function in Figure 8 for HT-TIIExHL-G-W distribution. It is evident from estimated cumulative distribution function (ECDF) and Kaplan-Meier (K-M) survival plots in Figure 11 that the introduced model closely matches the Europe covid-19 data. A TTT scaled plot displays a convex and then concave indicates a pattern of decreasing failure rate followed by increasing failure rate. Based on Figures 10 (a) and 10 (b) the developed model is a good fit to the heavily-skewed data.

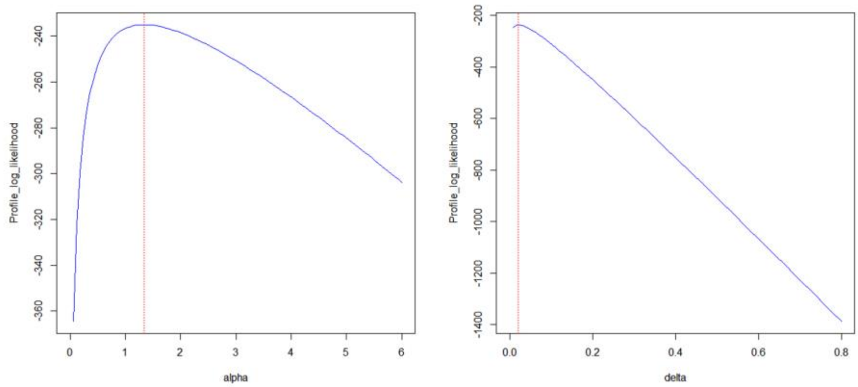

Figure 8
Plots of Profile log-likelihood function for Europe Covid 19 data

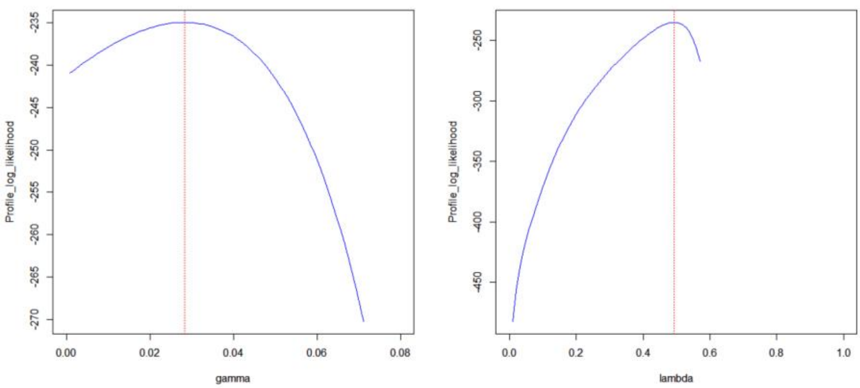

Figure 9
Plots of Profile log-likelihood function for Europe Covid 19 data

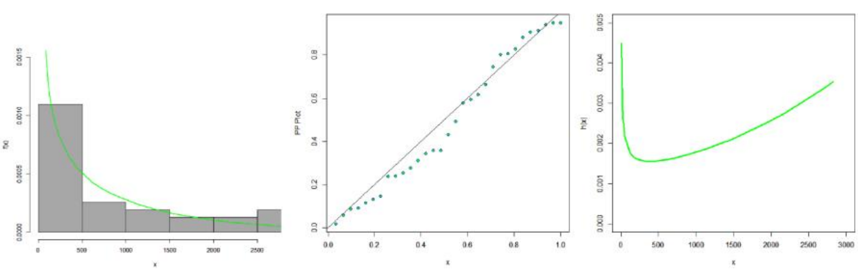

Figure 10
Fitted density, probability and hrf graphs for Europe Covid 19 data

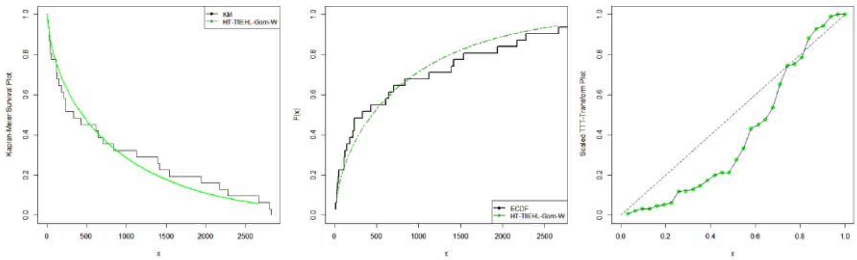

Figure 11
K-M survival, ECDF plots and TTT plot of the HT-TIIExHL-G-W distribution for the Europe COVID-19 data.

7.2 *Failure Times Data*

The data contains the number of hours that a machine from the Babel Tyres Factory in Iraq took to fail. (Visit the appendix for the observations). The estimated variance-covariance matrix is

$$\begin{bmatrix} 0.4768 & -0.0622 & 0.0173 & -0.0752 \\ -0.0622 & 0.0111 & -0.0015 & 0.0041 \\ 0.0173 & -0.0015 & 0.0015 & -0.0058 \\ -0.0752 & 0.0041 & -0.0058 & 0.0278 \end{bmatrix},$$

and the model parameters' 95% confidence intervals are $\alpha \in [0.7641 \pm 1.3534]$, $\sigma \in [0.1256 \pm 0.2062]$, $\omega \in [0.3445 \pm 0.0757]$ and $\lambda \in [0.5665 \pm 0.3268]$, respectively.

Table 6
MLE's and GoFs for several distributions fitted for failure times data set

Model	Estimates				Statistics							
	α	σ	ω	λ	$-2\log L$	AIC	$AICC$	BIC	W^*	A^*	$K-S$	$P-value$
HT-TIIExHL-G-W	0.7641	0.1256	0.3445	0.5665	327.7	335.7	337.3	341.1	0.0645	0.3546	0.1326	0.6876
	(0.6905)	(0.1052)	(0.0386)	(0.1668)								
	b	σ	λ	ω								
TLMOW	0.2673	0.9565	0.0004	1.2400	336.0	344.0	345.6	349.4	0.1271	0.7282	0.19801	0.2055
	(0.0751)	(0.0332)	(0.0006)	(0.2596)								
	ω	b	λ									
TLGW	2.8177×10^{-9}	4.5918	0.1243		381.7	387.7	388.7	391.8	0.0710	0.3879	0.5975	2.027×10^{-9}
	(0.0122)	(0.8648)	(0.0159)									
	a	b	α	θ								
TLWx	1.0021	0.0010	0.2349	1.0189	363.12	371.2	372.8	376.6	0.0703	0.3573	0.36698	0.0008
	(0.9076)	(0.0010)	(0.0430)	(0.2614)								
	b	β	σ	c								
EHL-OWTL-L	0.0283	0.0674	5.5701	1.6150	331.0	339.0	340.7	344.5	0.1285	0.9500	0.1832	0.2849
	(0.0362)	(0.0232)	(1.3664)	(0.6048)								
	α	ω	β									
HTBPTW	0.1095	1.5287	7.5012×10^{-5}		360.2	366.7	367.1	370.3	0.0885	0.3781	0.35758	0.0012
	(0.1800)	(0.3434)	(0.0004)									
	α	b	β	c								
EOWTLL	3.1003	0.0843	0.0437	2.1970	356.3	364.3	365.9	369.7	0.0675	0.3646	0.4371	3.077×10^{-5}
	(0.6019)	(0.0097)	(0.0040)	(0.0192)								

The Table 6 shows that the HT-TIIExHL-G-W model has superior to other distributions considered in terms of how well it fits the data. This is due to lower GoFs values and a higher K-S p-value. The graphs of the profile log-likelihood function in Figure 15 show the MLEs for the HT-TIIExHL-G-W model. The Kaplan-Meier survival and ECDF plots in Figure 13 show that the introduced model closely matches the failure times data. The TTT scaled plot in Figure 13 presents that the fitted hrf has a decreasing shape. Finally, the Figure 12 show that the dataset is heavily-tailed to the right, and the developed model is fitting the data well.

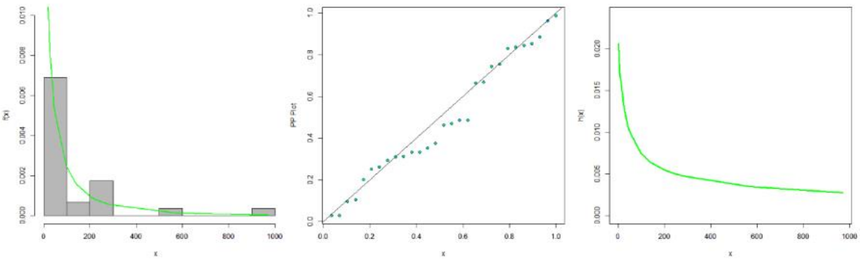

Figure 12
Fitted densities, probability and hrf plots for failure times data

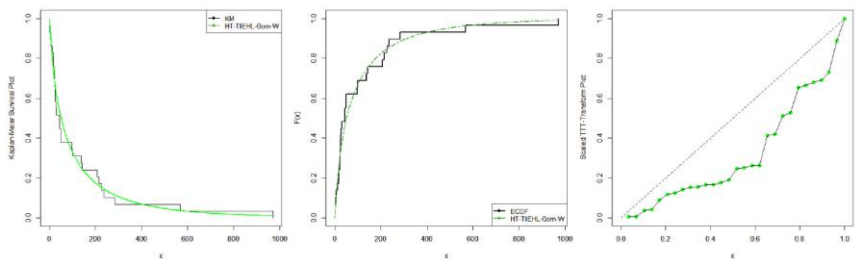

Figure 13
K-M survival, ECDF plots and TTT plot of the HT-TIIExHL-G-W distribution for the failure times data.

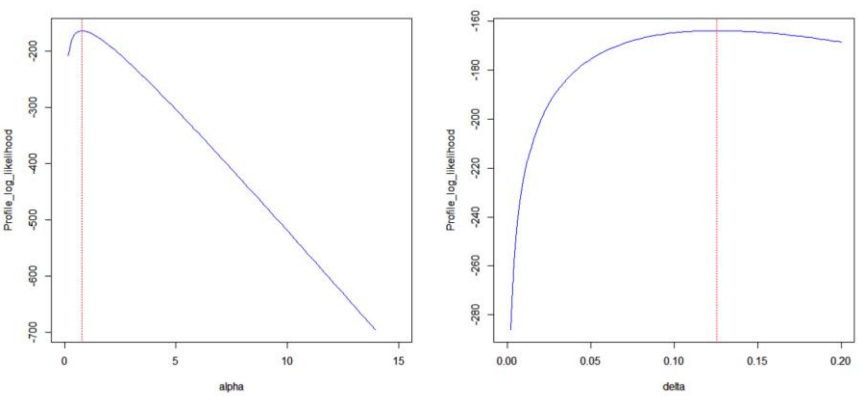

Figure 14
Graphs of Profile log-likelihood function for failure times data set

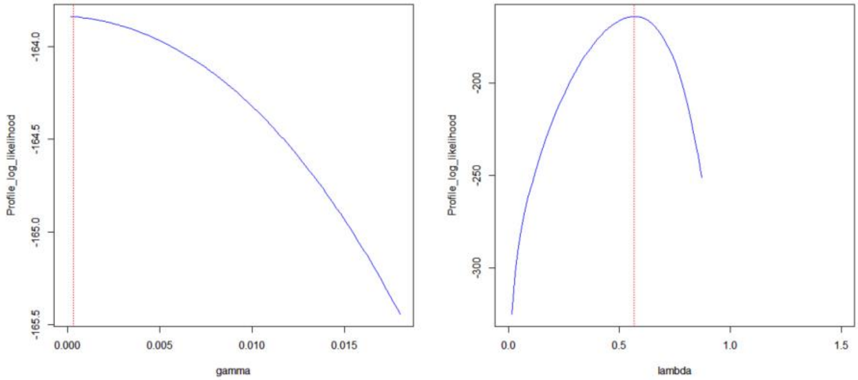

Figure 15
Graphs of Profile log-likelihood function for failure times data set

7.3 *China COVID-19 Data*

The third dataset displays the daily count of COVID-19-related fatalities in China recorded between 23 January 2022 to 28 March 2022. This data can be found on the Worldometers website (https://www.worldometers.info/coronavirus/country/china/). (Visit the appendix for the observations).

The estimated variance-covariance matrix is

$$\begin{bmatrix} 0.3111 & -0.0064 & 0.0002 & 0.0079 \\ -0.0064 & 0.0003 & 0.0003 & -0.0023 \\ 0.0002 & 0.0003 & 0.0011 & -0.0057 \\ 0.0079 & -0.0023 & -0.0057 & 0.0340 \end{bmatrix},$$

and the 95% confidence intervals for the model parameters are $\alpha \in [1.4714 \pm 1.0931]$, $\sigma \in [0.0225 \pm 0.0331]$, $\omega \in [0.0203 \pm 0.0635]$ and $\lambda \in [0.8048 \pm 0.3614]$, respectively.

Table 7
MLE's and GoFs for several distributions fitted for China Covid-19 data set

	Estimates				Statistics							
Model	α	σ	ω	λ	$-2\log L$	AIC	$AICC$	BIC	W^*	A^*	$K-S$	$P-value$
HT-TIIExHL-G-W	1.4714	0.0225	0.0203	0.8048	640.9	648.9	649.6	657.7	0.0705	0.5234	0.0860	0.7133
	(0.5577)	(0.0169)	(0.0324)	(0.1844)								
	b	σ	λ	ω								
TLMOW	0.8101	1.1619	0.0038	1.2169	646.9	654.9	655.6	663.6	0.1082	0.7941	0.0894	0.6669
	(1.0370)	(1.0718)	(0.0202)	(1.0198)								
	ω	b	λ									
TLGW	3.6848×10^{-9}	4.2917	0.1407		812.7	818.7	819.1	825.3	0.1201	0.8729	0.6491	2.2×10^{-16}
	(0.0147)	(0.5363)	(0.0122)									
	a	b	α	θ								
TLWx	0.0840	25.2640	29.9930	0.1170	642.5	650.5	651.2	659.3	0.1226	0.8047	0.1129	0.3692
	(0.0007)	(1.0576×10^{-5})	(6.3645×10^{-5})	(0.1505)								
	b	β	σ	c								
EHL-OWTL-L	10.8493	1.9872	0.6205	0.2811	645.8	653.8	654.5	662.6	0.1045	0.7571	0.0893	0.6687
	(3.9962)	(0.9198)	(0.3342)	(0.0570)								
	α	ω	β									
HTBPTW	0.1162	1.5120	0.0001		764.8	770.8	771.1	777.3	0.1196	0.8719	0.4571	2.1×10^{-12}
	(0.0133)	(0.2423)	(0.0004)									
	α	b	β	c								
EOWTLL	9.3283	0.7098	0.0519	2.8794	659.0	667.0	667.6	675.7	0.1239	0.8967	0.1421	0.1392
	(1.3927)	(0.7093)	(0.0313)	(1.6655)								

The findings presented in Table 7, it is clearly shown that the HT-TIIExHL-G-W distribution exhibits the most favorable GoFs, characterized by the lowest values, when compared to the various models examined in this study. Furthermore, it recorded higher p-value from Kolmogorov-Smirnov (K-S) statistic, further highlighting its better fit among the models under consideration in this paper. Thus, we draw the conclusion that the HT-TIIExHL-G-W model fit the China covid-19 data better than the several selected distributions. The mles of the proposed model are shown by the graphs of the profile log-likelihood function in Figure 16. The Kaplan-Meier survival and ECDF plots are displayed in Figure 18, which shows that the introduced model fits these plots very closely. TTT scaled plot is shown in Figure 18, that is, first concave and then convex indicates a pattern of upside bath-tub followed by bath-tub of an hrf. As well, Figure 17 (a) and 17 (b) we can conclude that the data set is heavily-tailed to the right.

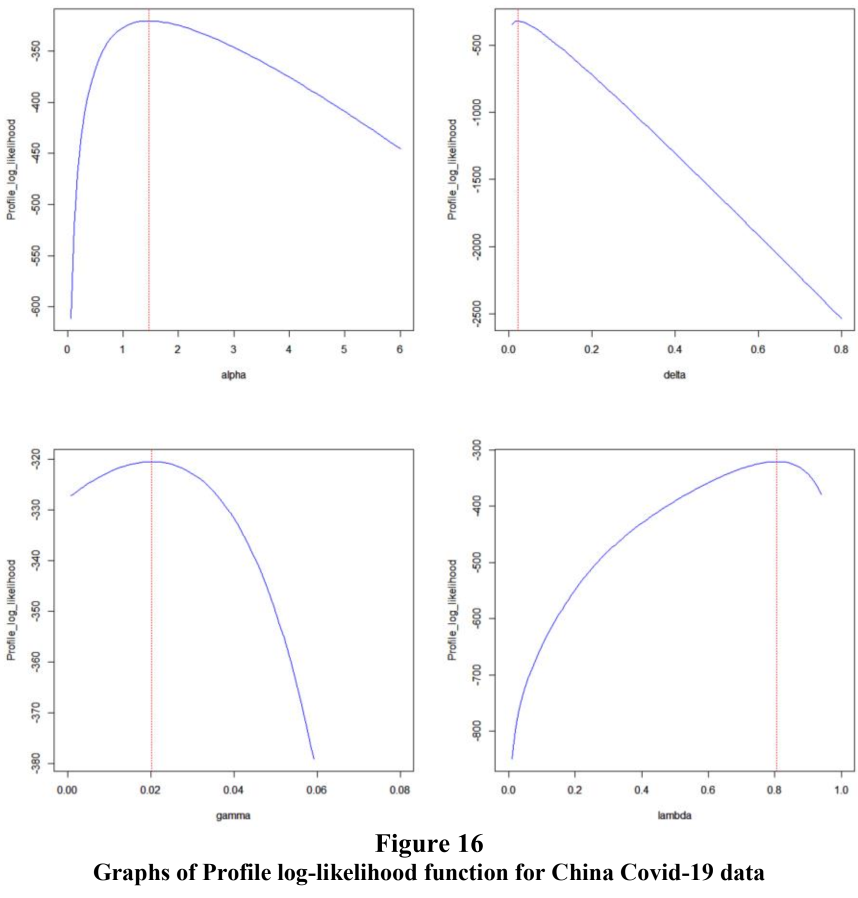

Figure 16
Graphs of Profile log-likelihood function for China Covid-19 data

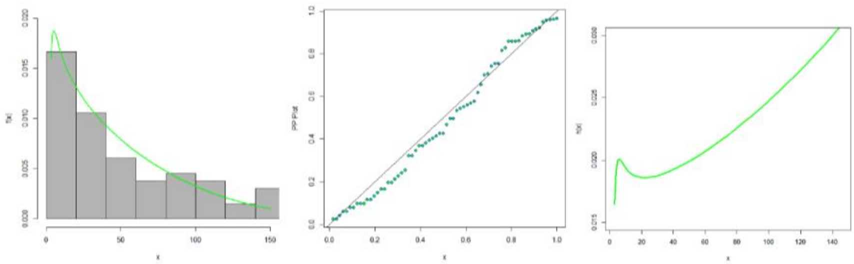

Figure 17
Fitted densities, probability and hrf graphs for China covid-19 data

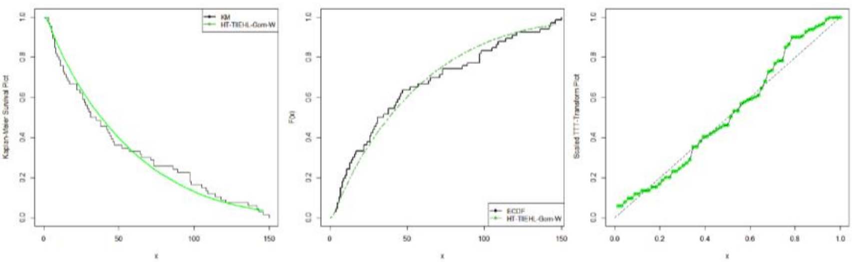

Figure 18
K-M survival, ECDF plots and TTT plot of the HT-TIIExHL-G-W distribution for the China covid-19 data set.

8. Concluding Remarks

We have presented a new family of probability distributions known as the HT-TIIExHL-G-G distribution. This newly proposed distribution exhibits the capacity to effectively handle data with heavy tails, while accommodating both non-monotonic and monotonic hrf shapes. It is tractable and has desirable properties. Its expression can be represented as an infinite linear combination of Exp-G distributions. We explored various parameter estimation methods for the HT-TIIExHL-G-G distribution, with consistency in parameter estimation demonstrated through a simulation study involving varying sample sizes. The practical applications provided showed the better performance of the HT-TIIExHL-G-G distribution when in contrast to non-nested distribution. This is supported in the results presented in Tables 5, 6 and 7, which demonstrate the favorable GoFs and Kolmogorov-Smirnov p-values associated with this distribution across three different data examples.

Appendix

The URL provides the derivations of the statistical properties, probability density functions (pdfs) of the competing models and data examples considered in this work.

https://drive.google.com/file/d/1qwu0Mj7Zw2ufsY-oBsIHPKzAC3cwK8l P/view?usp=sharing

References

[1] A. Algarni, A. M. Almarashi, I. Elbatal, M. A. Hassan, E. Almetwally, A. Daghistani, and M. Elgarhy, “Type I Half Logistic Burr X-G Family: Properties, Bayesian, and Non Bayesian Estimation Under Censored Samples and Applications to COVID-19 Data,” *Mathematical Problems in Engineering*, vol. 2021, pp. 1–21 (2021), doi: 10.1155/2021/5461130.

[2] M. Alizadeh, G. M. Cordeiro, G. Pinho, and I. Ghosh, “The Gompertz-G Family of Distributions,” *Journal of Statistical Theory and Practice*, vol. 11, no. 1, pp. 179–207 (2017).

[3] S. Chamunorwa, B. Oluyede, T. Moakofi, and F. Chipepa, “The Type II Exponentiated Half Logistic-Gompertz-G Power Series Class of Distributions: Properties and Applications,” *Statistics, Optimization & Information Computing,* vol. 12, no. 2, pp. 381–399 (2024), doi: 10.19139/soic-2310-5070-1721.

[4] G. Chen and N. Balakrishnan, “A General Purpose Approximate Goodness-of-Fit Test,” *Journal of Quality Technology*, vol. 27, no. 2, pp. 154–161 (1985).

[5] K. Dutta and J. Perry, “A Tale of Tails: An Empirical Analysis of Loss Distribution Models for Estimating Operational Risk Capital,” (2006). [Online]. Available: (Add URL if available).

[6] B. Gompertz, “On the Nature of the Function Expressive of the Law of Human Mortality and on the New Mode of Determining the Value of Life Contingencies,” *Philosophical Transactions of the Royal Society of London*, vol. 115, pp. 513–580 (1825).

[7] S. Harini, M. Subbiah, and M. R. Srinivasan, “Fitting Length of Stay in Hospitals Using Transformed Distributions,” *Communications in Statistics: Case Studies, Data Analysis and Applications,* vol. 4, no. 1, pp. 1–8 (2017).

[8] A. Ickowicz and R. Sparks, “Modelling Hospital Length of Stay Using Convolutive Mixtures Distributions,” *Statistics in Medicine*, vol. 36, no. 1, pp. 122–135 (2017), doi: 10.1002/sim.7148. PMID: 27704639.

[9] B. Oluyede, S. Chamunorwa, F. Chipepa, and M. Alizadeh, “The Topp-Leone-Gompertz-G Family of Distributions with Applications,” *Journal of Statistics and Management Systems,* vol. 25, no. 6, pp. 1399–1423 (2021), doi: 10.1080/09720510.2021.1972623.

[10] B. Oluyede and T. Moakofi, “Type II Exponentiated Half-Logistic-Gompertz-Topp-Leone-G Family of Distributions with Applications,”

Central European Journal of Economic Modelling and Econometrics, vol. 14, pp. 415–461 (2022).

[11] K. Rannona, B. Oluyede, and S. Chamunorwa, "The Gompertz-Topp Leone-G Family of Distributions with Applications," *Journal of Probability and Statistical Science,* vol. 20, no. 1, pp. 108–126 (2022).

[12] C. E. Shannon, "Prediction and Entropy of Printed English," *The Bell System Technical Journal*, vol. 30, pp. 50–64 (1951).

[13] J. Zendehdel, R. Zarei, and S. M. Mahmoudi, "A New Generalized Weibull-Gompertz Distribution and Its Properties," *Journal of Statistics and Management Systems*, vol. 25, no. 4, pp. 837–856 (2022), doi: 10.1080/09720510.2021.1938997.

[14] J. Zhao, Z. Ahmad, E. Mahmoudi, E. Hossam, and M. M. M. El-Din, "A New Class of heavy-tailed Distributions: Modelling and Simulating Actuarial Measures," *Complexity*, pp. 1–18 (2021), doi: 10.1155/2021/5580228.

[15] W. Zhao, S. K. Khosa, Z. Ahmad, M. Aslam, and A. Z. Afify, "Type-I heavy-tailed Family with Applications in Medicine, Engineering and Insurance," *PLoS ONE*, vol. 15, no. 8, e0237462 (2020), doi: 10.1371/journal.pone.0237462.

Received January, 2024